Pushing the Limits of Small Period Permanent Magnet Undulators

Johannes Bahrdt, HZB, FEL Conference, Shanghai, China, August, 2011

Pushing the limits in various directions...

HZB Helmholtz Zentrum Berlin

- Undulators for X-FELs
- Magnet material development
- Cryogenic undulators
- Sub-cm period devices
- Measurememt equipment

Challenges of long undulators for X-FELs

HZB Helmholtz Zentrum Berlin

Out of vacuum:

- Trajectory shimming over 5m length, conventional granite bench
- Tight mechanic tolerances (magnetic gap, Taper) over 5m
- Motion control, synchronisation of several dozens of modules
- More complexicity added with APPLE II undulators

In-Vacuum

- Trajectory shimming over 5m length with new measurement systems
- Mechanic rigidity under vacuum
- In-vacuum gap measurement system
- Motion control, synchronisation of several dozens of devices

LCLS Fixed Gap Undulators

HZB Helmholtz Zentrum Berlin

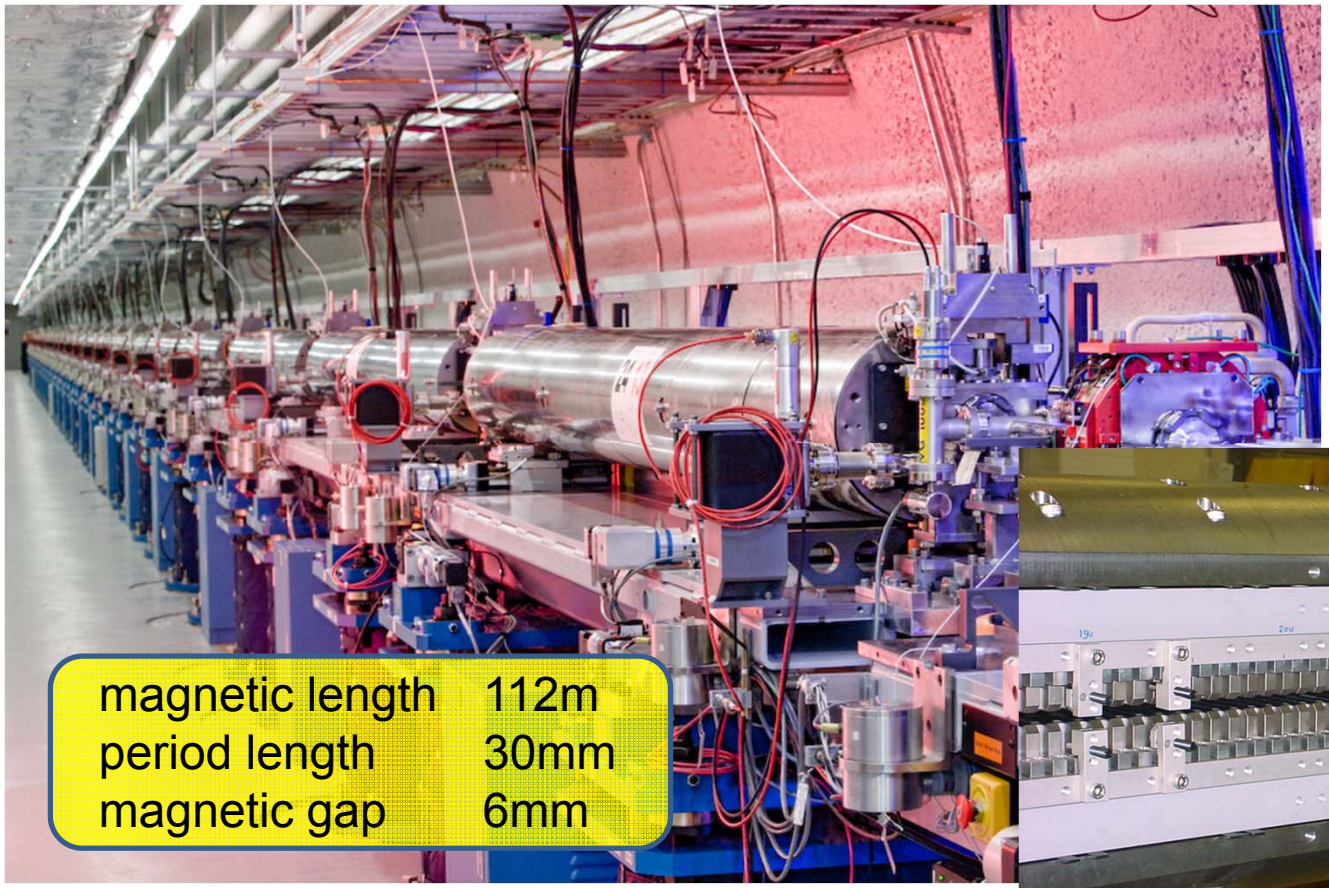

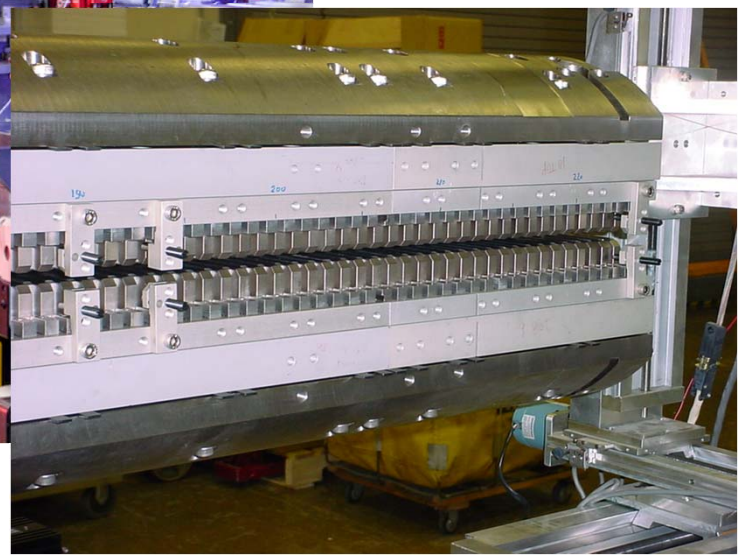

Courtesy of S. Sasaki

Next steps:

- self seeding
- 2nd harmonic afterburner
- variable gap
- variable polarization

European XFEL Planar Undulators

HZB Helmholtz Zentrum Berlin

5m Prototype module at measurement bench

Courtesy of J. Pflüger

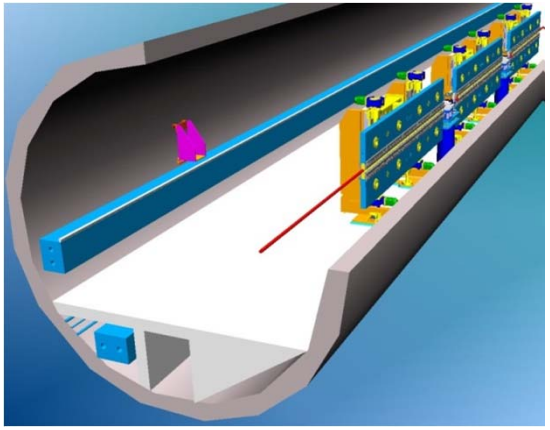

magnetic length	175m
period length	40mm
minimum gap	10mm

SPRING-8 XFEL In-Vacuum Undulators

HZB Helmholtz Zentrum Berlin

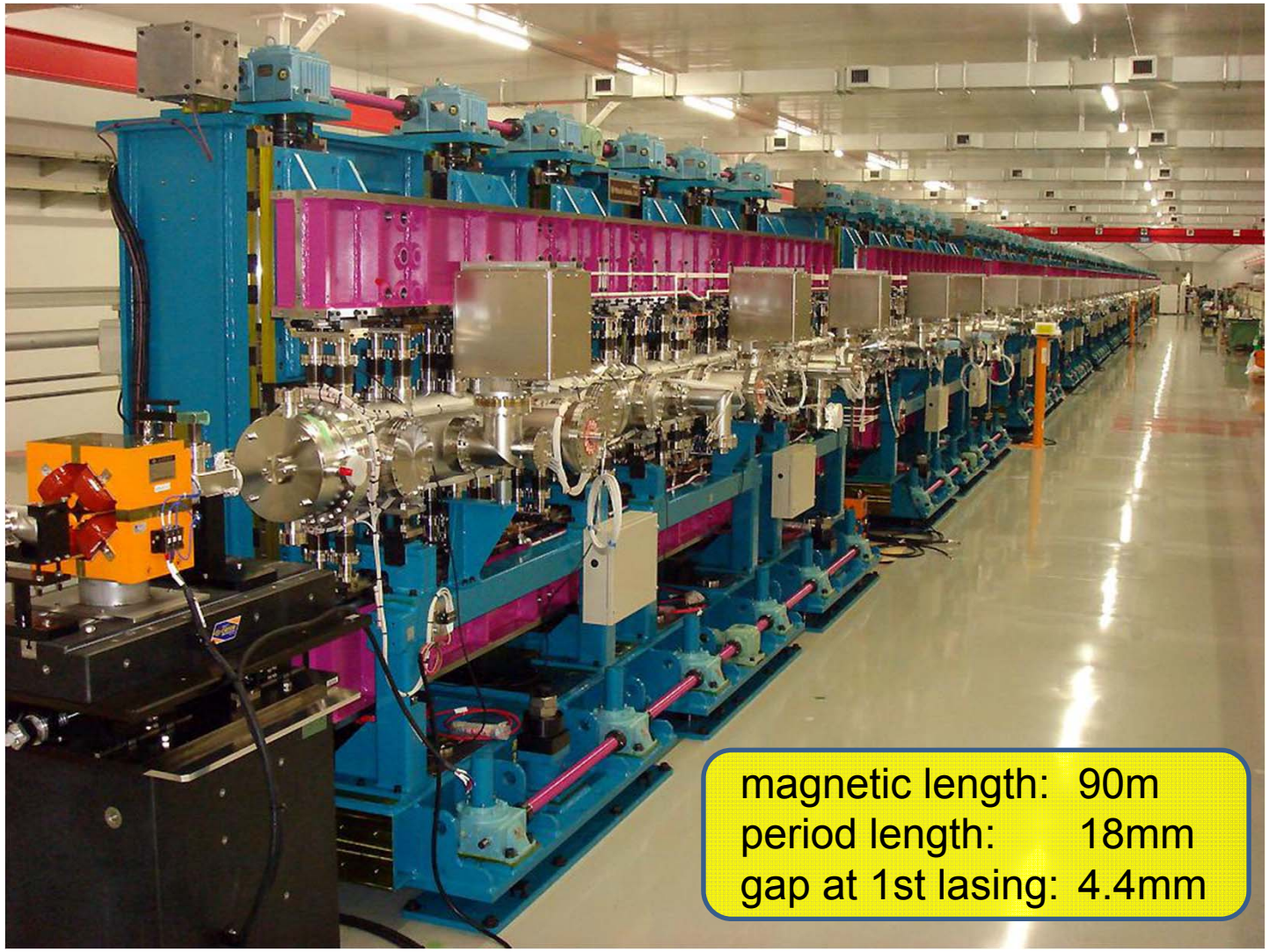

Courtesy of T. Tanaka

PETRA III APPLE II Undulator as built at HZB

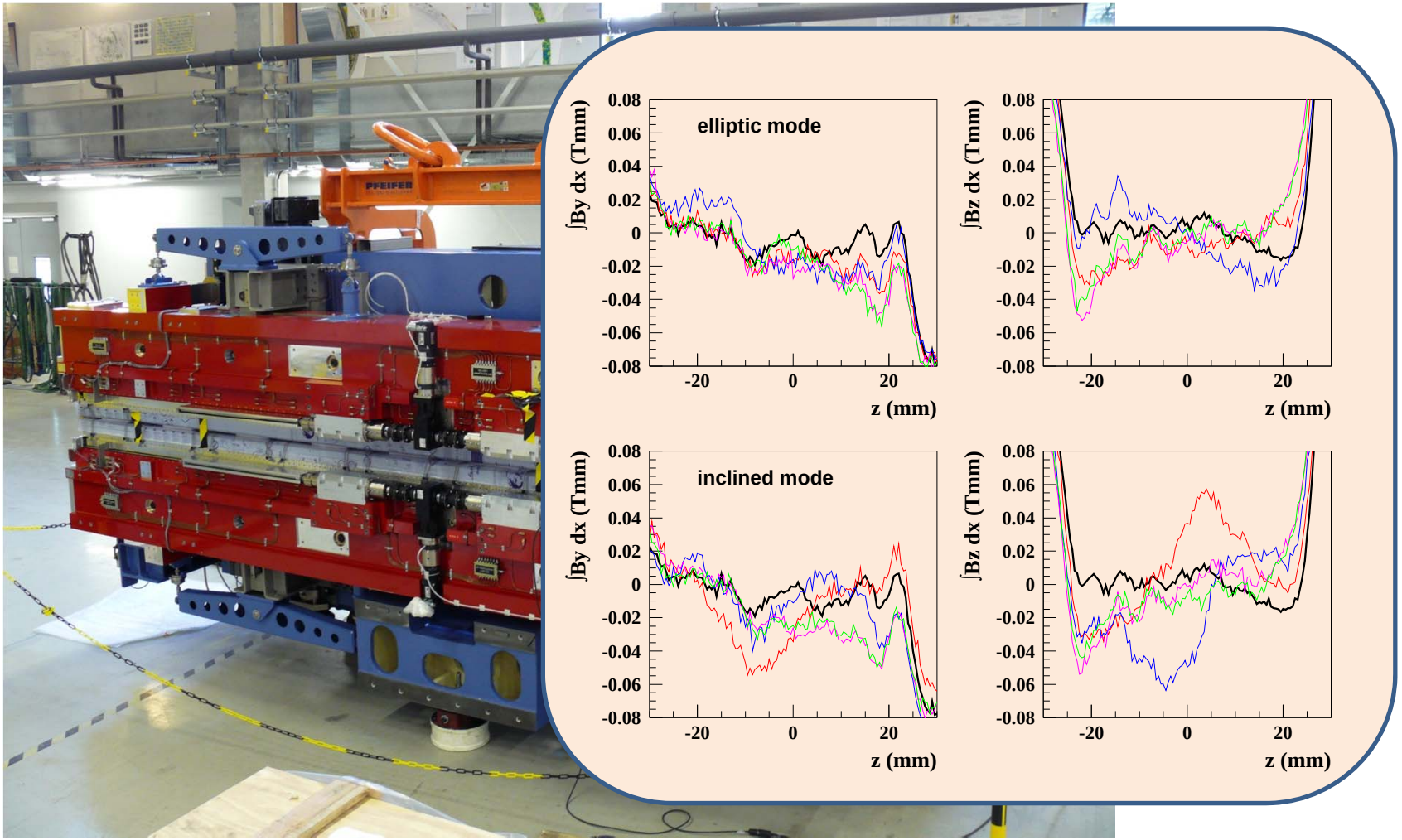

J. Bahrdt et al., EPAC2008, SRI 2009, IPAC 2011

Advanced Variably Polarizing Undulators

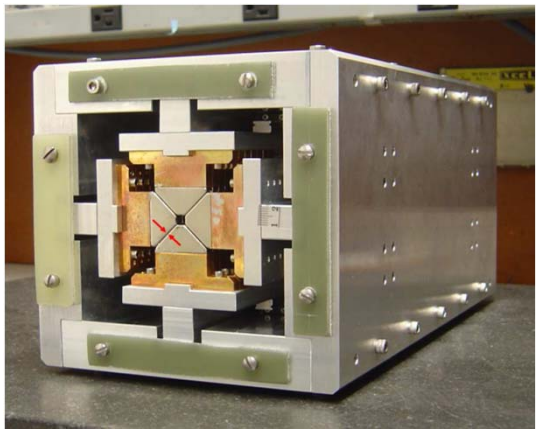

A. Temnykh, PRST-AB, 11, 120702 (2008)

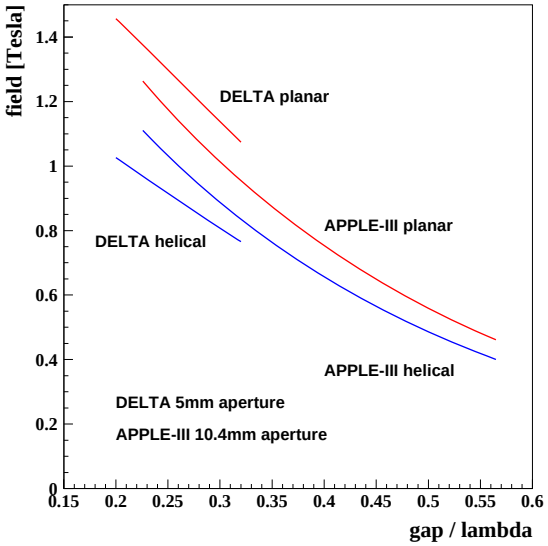

Currently under discussion
2nd harmonic afterburner

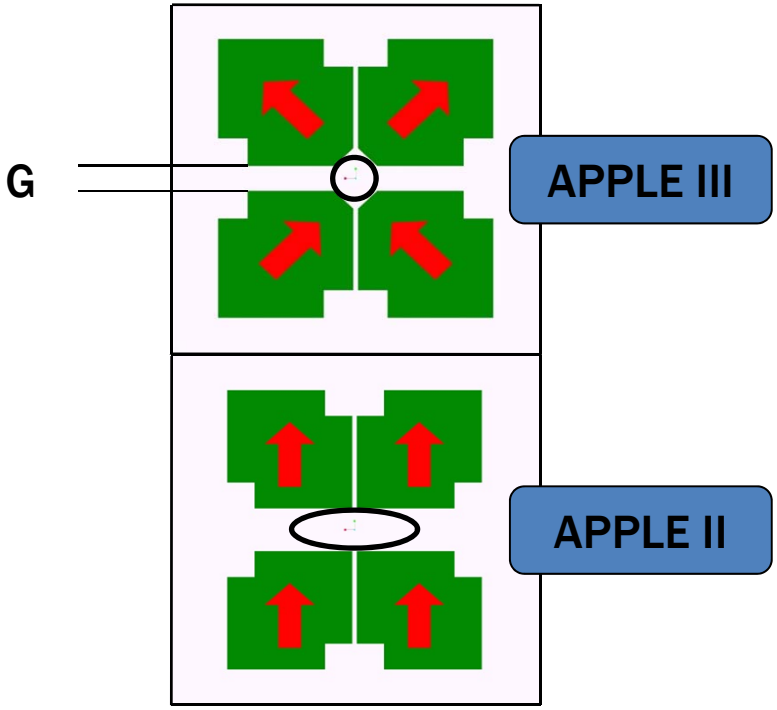

J. Bahrdt et al., Proc. of FEL Conf., Trieste, Italy (2004) 610-613

Small Period / Small Gap Devices

HZB Helmholtz Zentrum Berlin

SACLA: first lasing at 4.4mm gap
minimum gap = 3.5mm
λ=18mm

SWISS FEL: minimum gap = 3.2mm
λ=15mm

Prototyping for Laser Plasma Acelerator, Group of F. Gruener

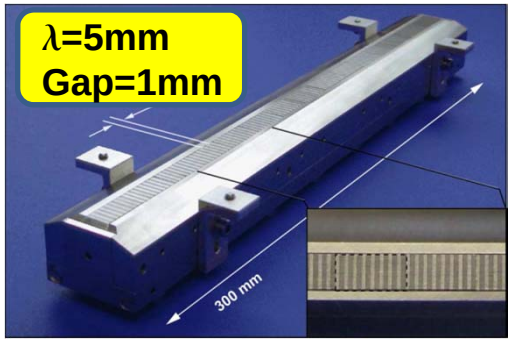

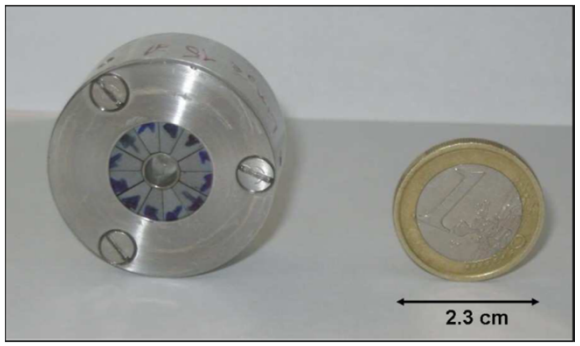

*T. Eichner et al., Phys. Rev. Spec. Topic. AB, **10**, 082401 (2007) 1-9.*

Collaboration between LMU-Munich and HZB
Further prototypes exmploying:
- cryogenic design
- new materials
- challenging magnet design

HZB Helmholtz Zentrum Berlin

Remanence

$$B_r(20°C) = B_{r-sat}(20°C) \cdot \frac{\rho}{\rho_0} \cdot (1 - V_{nonmagnetic}) \cdot f_\varphi$$

$$f_\varphi = \cos(\varphi)$$

$$\varphi = \arctan\left(2\frac{B_{r-perp}}{B_{r-par}}\right)$$

Current status:

- $\rho/\rho_0 > 0.995$, is achieved with the so-called liquid phase sintering
- $f_\varphi > 0.98$, high alignment factor, sophisticated timing during pressing
- Non-magnet particles typical < 4%

Example: energy product of Nd2Fe17B

Theory: 509 kJ/m^3 ⟷ Achieved: 469 kJ/m^3

Not much space for improvement for known materials

Material development: Coercivity I

Coercivity Hcj still one order of magnitude below theory

„Brown‘s paradoxon“

Many reasons (Kronmüller)

- non-magnetic extended grains between magnetic grains
- misoriented grains
- missing grain boundary surfaces resulting in large grains
- extended transition regions of tilted crystal structures between grains

R & D ongoing:

- Optimizing the microcrystalline structure, grain size, alignment angle
- Dy enriched powder
- Two alloy method (Shin-Etsu)
- Grain Boundary Diffusion (GPD)

Material development: Coercivity II

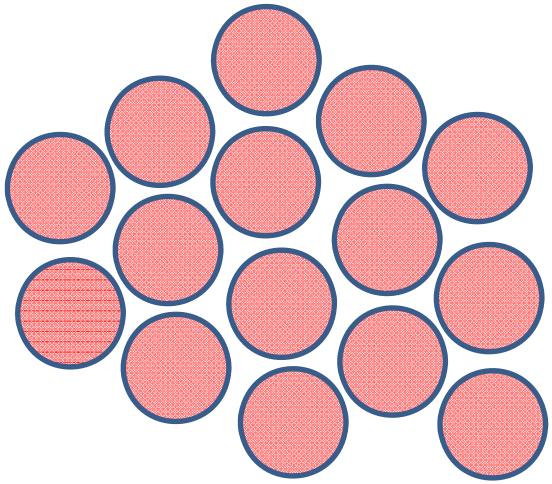

grades differ in amount of Dy in grain bulk

Procedure:
add Dy to powder before pressing

- gain in coercivity
- loss in remanence

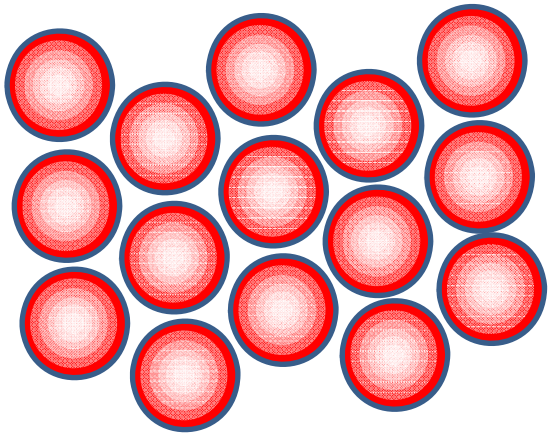

slight Dy gradient to grain boundaries

Procedure:
Two alloy method (Shin-Etsu)

- gain in coercivity
- smaller loss in remanence

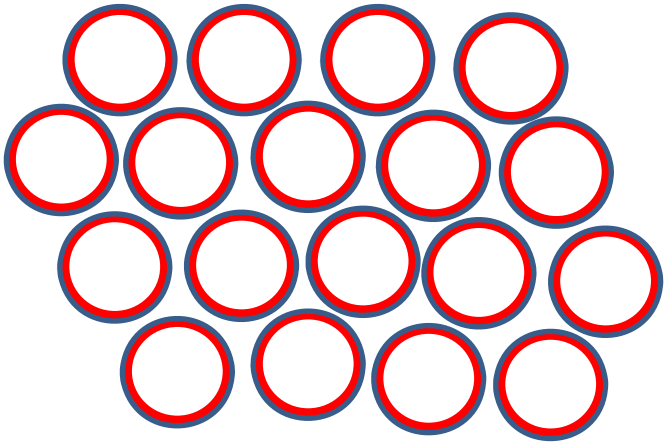

sharp concentration peak of Dy at grain boundary

Procedure:
Grain Boundary Diffusion (GPD)

- higher coercivity
- no loss in remanence

HZB Helmholtz Zentrum Berlin

Grain Boundary Diffusion (GPD)

Known already for 10 years, now commercially avalilable

- Coating of magnets with Dy or Tb (expensive)
- Heating the magnets to 800-900 degrees
- Fast diffusion of Dy in liquid phase (boundary)
- Slow diffusion from boundary into the bulk
- Thin highly enriched Dy shells around grain

- Depth profile: $\Delta H_{cj} = Ae^{-x^2/d^2}$
- Penetration depth of Dy about d = 2.2mm

H. Nakamura et al., J. Phys. D: Appl. Phys. 44 (2011) 064004-1-5.

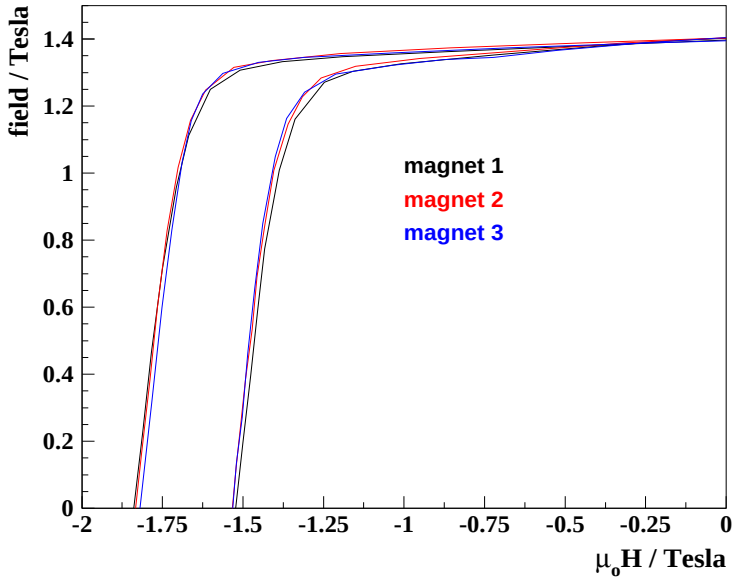

PrFeB samples before / after GBD
Courtesy of Vacuumschmelze

Extremely useful for
high end small period devices

Why Cryogenic Undulators?

HZB Helmholtz Zentrum Berlin

Advantage of Cryogenic Devices:
- gain in remanence, larger tuning range for small period IDs
  stability recovered at low temperatures
- less sensitive on thermal dependence of magnetic properties

Advantage of PrFeB Undulators
- no spin reorientaion at 135K, lower temperatures possible
- cooling with liquid N2, no heating necessary
- gain in stability (coercivity), though, gain declines at low temperatures
  due to decreasing thermal capacity (zero at 0K)

Availability of PrFeB
- ingredients comparable prices as for NdFeB
- however, more expensive due to small number of customers
- melting batch 1-2 to, powder batch 500kg
- laboratory batch: 30kg, reproducability, performance incr. with batch size

Existing devices: **ESRF, PSI, DIAMOND, SOLEIL (PrFeB)**
Installed: **ESRF, PSI, (soon SOLEIL)**

First Spectra from SLS / PSI Device

PAUL SCHERRER INSTITUT

HZB Helmholtz Zentrum Berlin

Marco Calvi, Thomas Schmidt, Antonio Cervellino, Phil Willmott

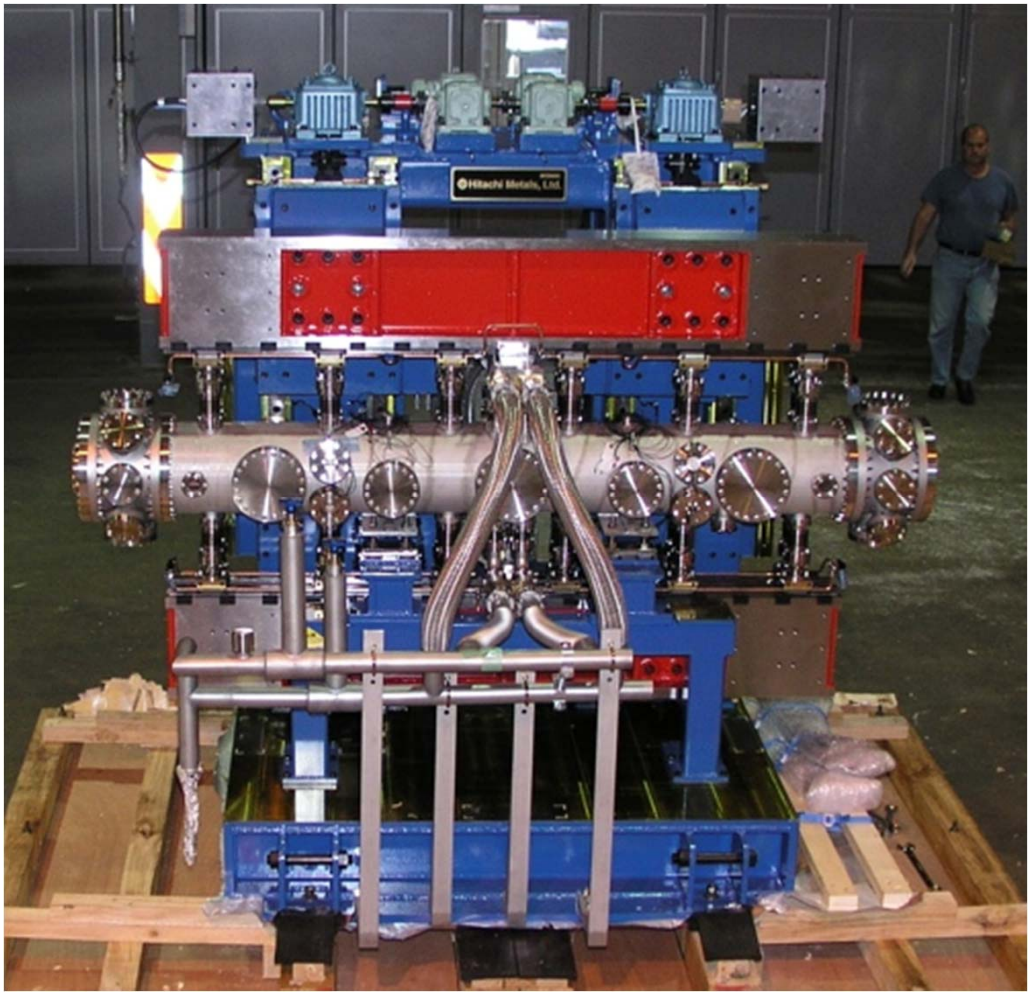

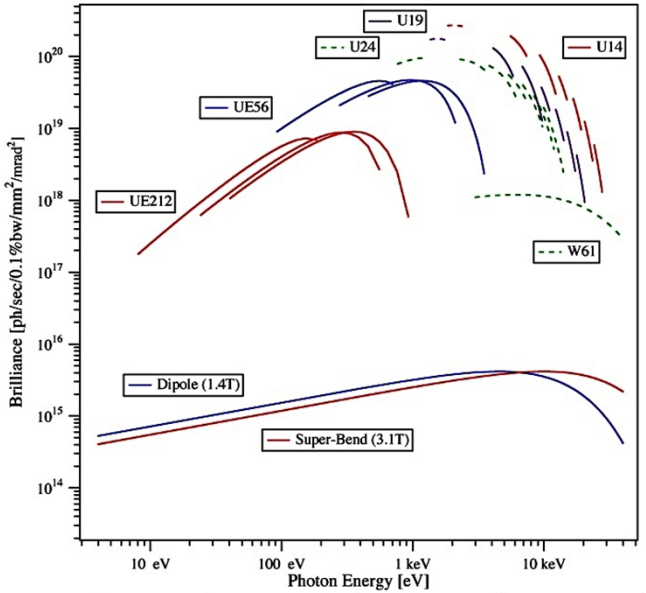

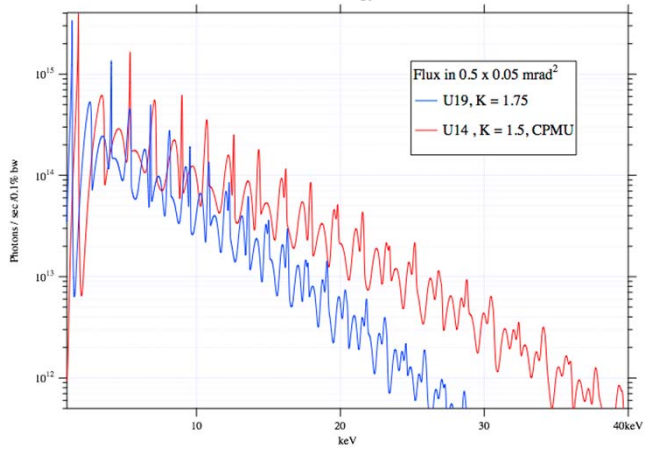

Spin Reorientation

Anisotropy energy

$$E = K_1 sin^2(\vartheta) + K_2 sin^4(\vartheta)$$

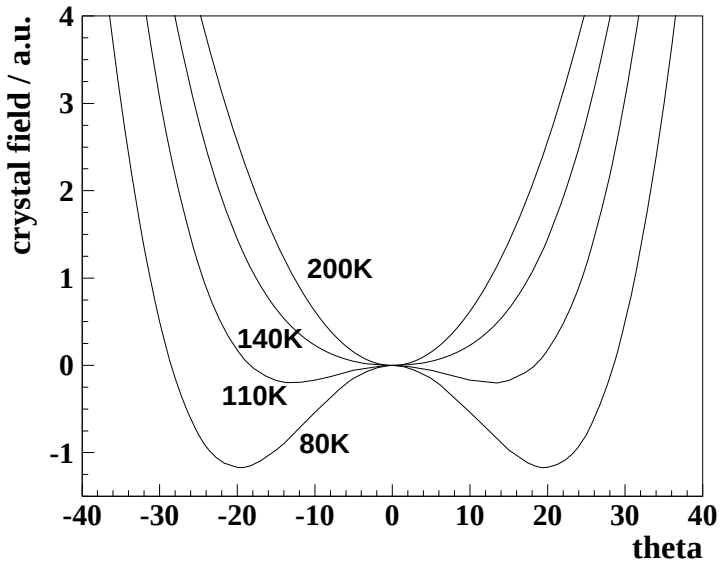

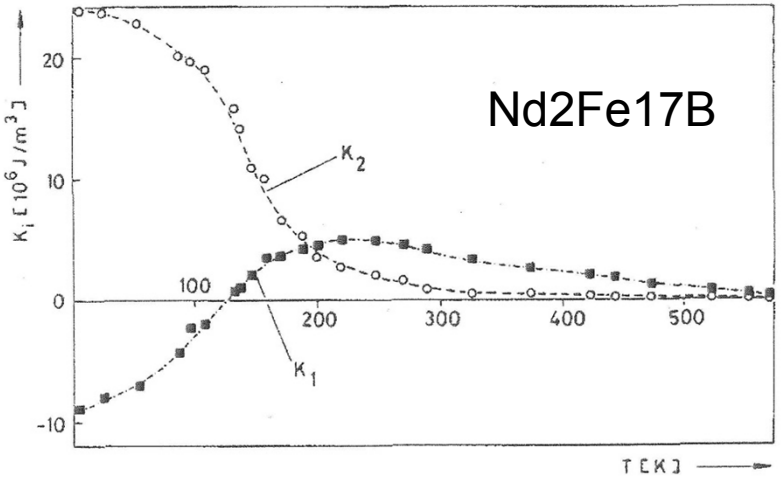

K.-D. Durst, H. Kronmueller,
J. Mag. And Mat. 59 (1986) 86-89

Implementation of these equations in RADIA:
G. Le Bec, J. Chavanne, C. Benabderrahmane,
Proc. of PAC, Vancouver, BC, Canada (2009) 327-329

Material Development: PrFeB

New PrFeB grade as developed by VAC, raw data

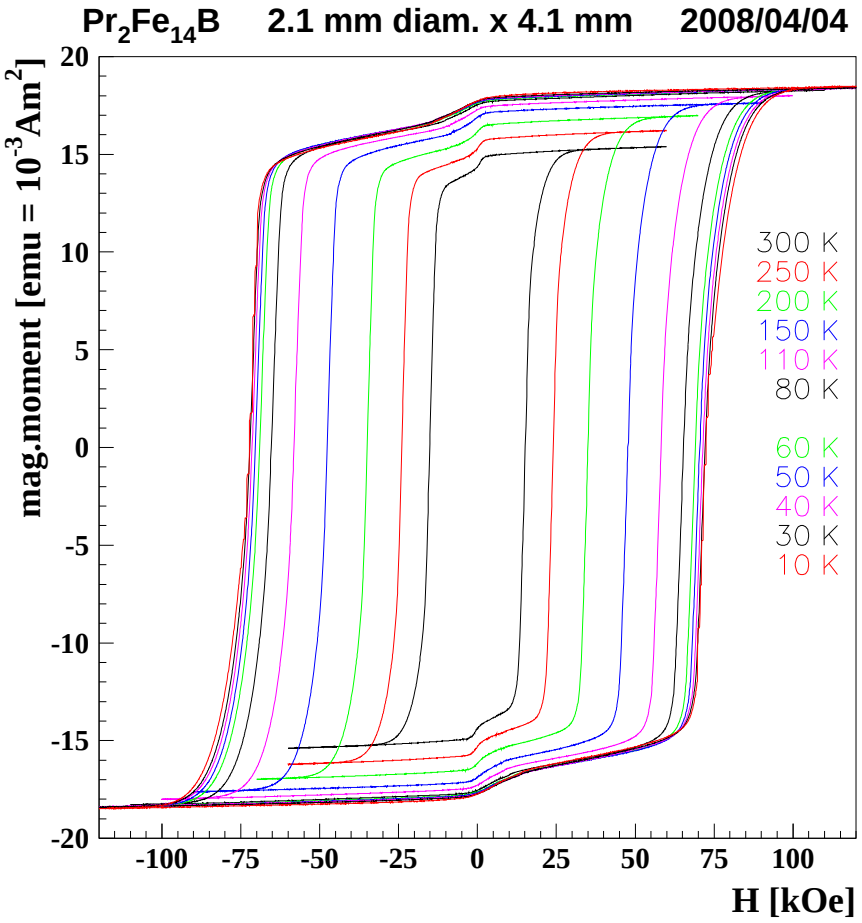

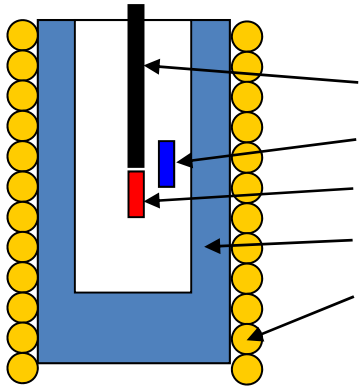

motor drive system
pickup coil
vibrating magnet sample
He bath cryostate
SC solenoid

Analysis requires:
- demagnetization factors
- surface model

Fitting of Magnetic Data

HZB Helmholtz Zentrum Berlin

fitting model

$$M = J_{bulk} \cdot bulk\_volume + J_{side} \cdot side\_volume + J_{pole} \cdot pole\_volume$$

$$J_{bulk}(H_{bulk}) = \sum_{i=1}^{3} J_i \cdot \tanh\left(\frac{\xi_i \cdot \mu_0}{J_i} (H_{bulk} - H_{cj}) \right) + F$$

$$H_{bulk} = H_{ext} - (D \cdot J_{bulk}(H_{bulk}))/\mu_0$$

with

$$F = \mu_0 \cdot \chi_0 \cdot (H_{bulk} - H_{cj}) \quad \text{for} \quad H_{bulk} \le H_{cj1}$$

$$F = \mu_0 \cdot \chi_0 \cdot (H_{cj1} - H_{cj}) + \mu_0 \cdot \chi_{01} \cdot (H_{bulk} - H_{cj1}) \quad \text{for} \quad H_{bulk} > H_{cj1}$$

$$J_{pole} = B_{bulk} = J_{bulk} + \mu_0 H_{bulk}$$

$$J_{pole} = |J_{bulk}(0)| \frac{B_{bulk}}{|B_{bulk}|}$$

for $|B_{bulk}| \le |J_{bulk}(0)|$ and $|B_{bulk}| > |J_{bulk}(0)|$

$$J_{side} = J_{bulk}(0) \frac{H_{bulk} - H_{cj1}}{|H_{bulk} - H_{cj1}|}$$

12 Fitting parameters $J_1, J_2, J_3, \xi_1, \xi_2, \xi_3, \chi_0, \chi_1, H_{cj}, H_{cj1}, d_s, d_p$

J. Bahrdt et al., SRI 2009, AIP Conf. proc. 1234, p499-502

PrFeB-Material as Developed by VAC

Results from fit:

- energy product (BH)max @ 85 K = 520 kJ/m^3
- B_r(10K)=1.7T
- Hcj=73kOe

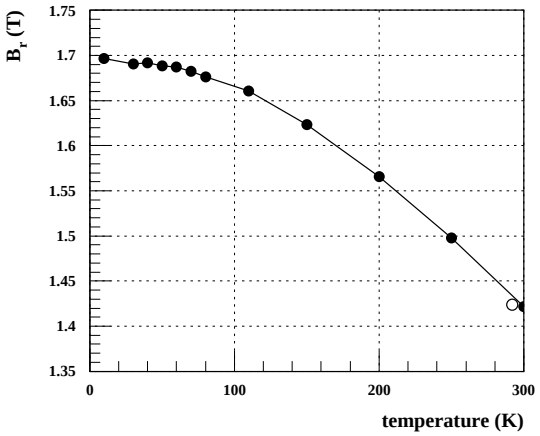

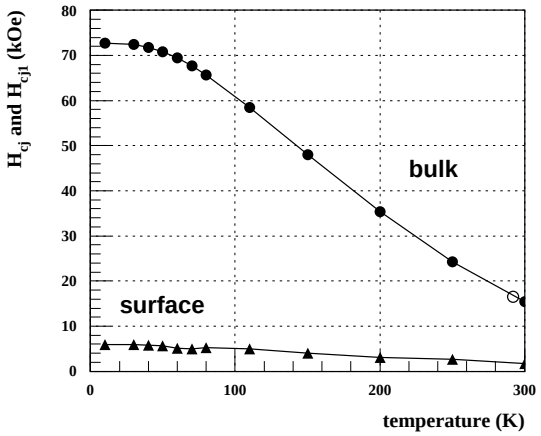

K. Üstüner et al., 20th Conference on Rare Earth Permanent Magnets, Crete 2008

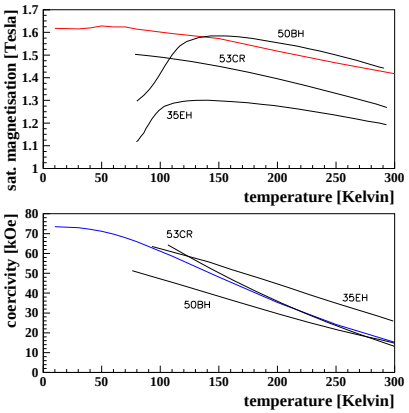

Comparison with other magnet grades

Magnetic Design of HZB-LMU Prototype

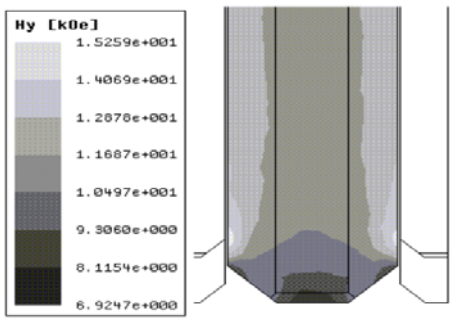

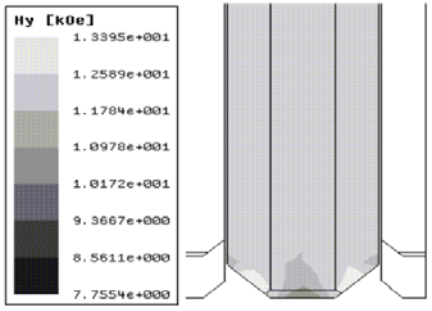

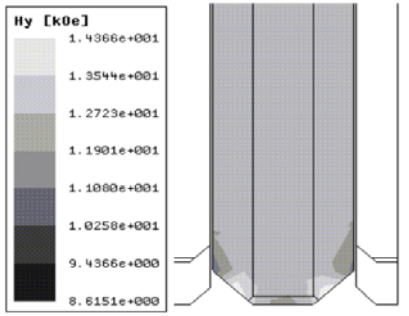

high reverse fields at pole tips
even higher reverse fields during assembly

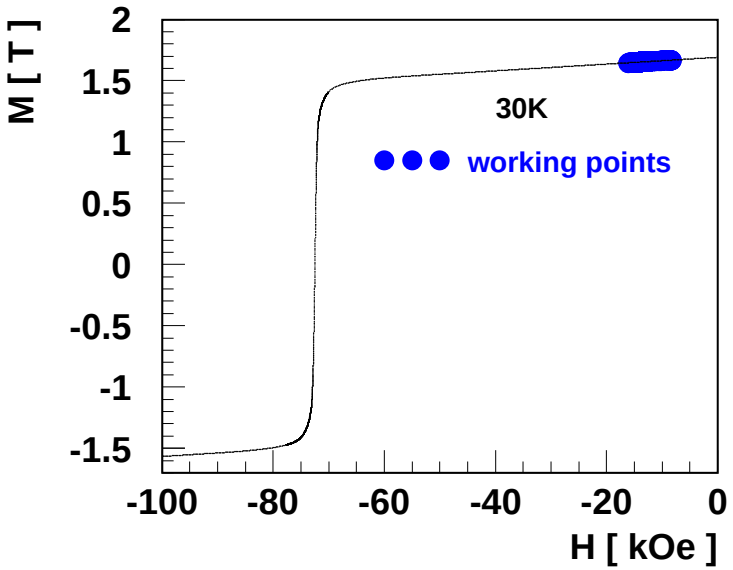

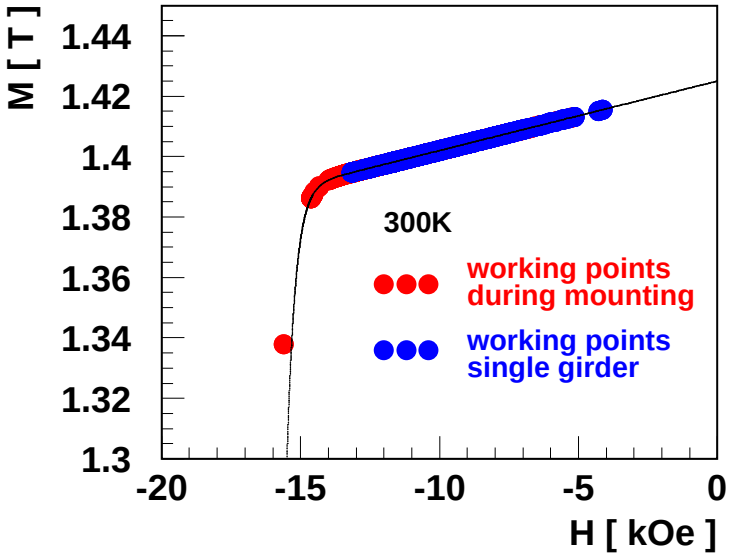

Assembly and First Test with Beam

HZB Helmholtz Zentrum Berlin

Many thanks to Tasso

LYKOS

-22°C
Huge Windchill-Factor!
(when the fans are blowing)

Fixed gap device

Magnet material:	PrFeB
Pole material:	CoFe
Design:	Hybrid
Period length:	9mm
Period number:	20

Field gain at low temperatures: 15%

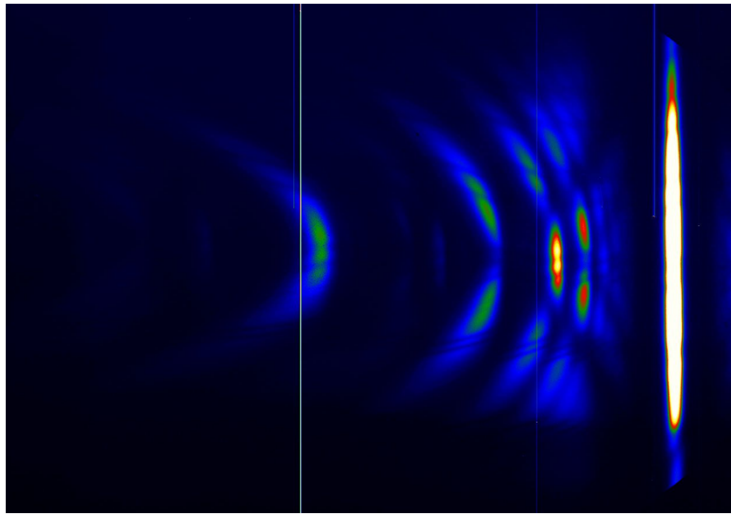

First spectrum taken at MAMI, 850 MeV
Transmission grating, F. Holy et al.

HZB Helmholtz Zentrum Berlin

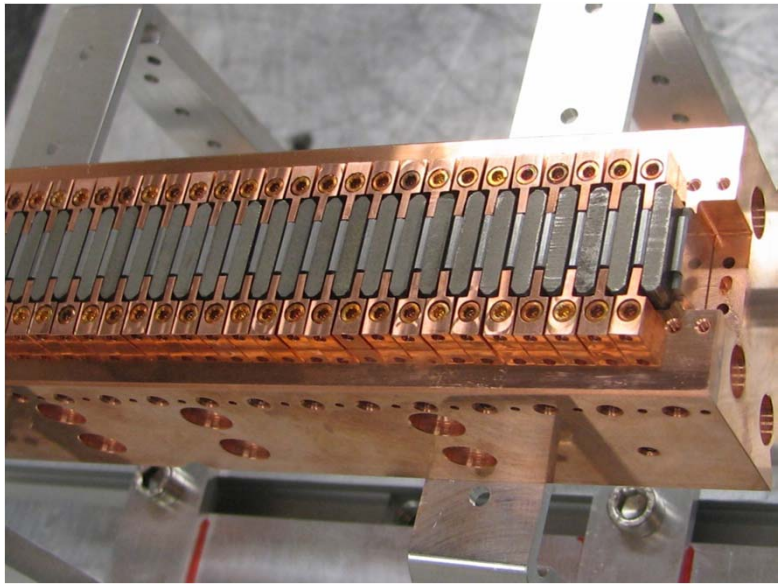

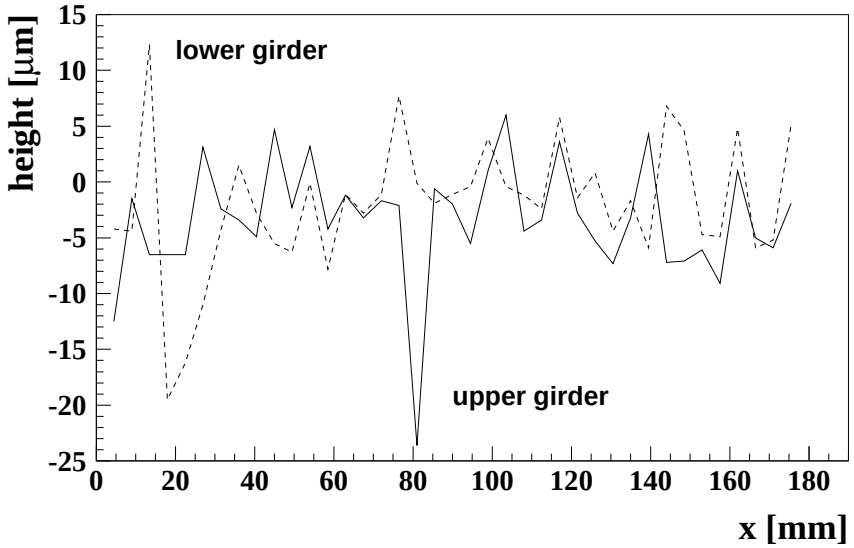

Pole heights after initial assembly

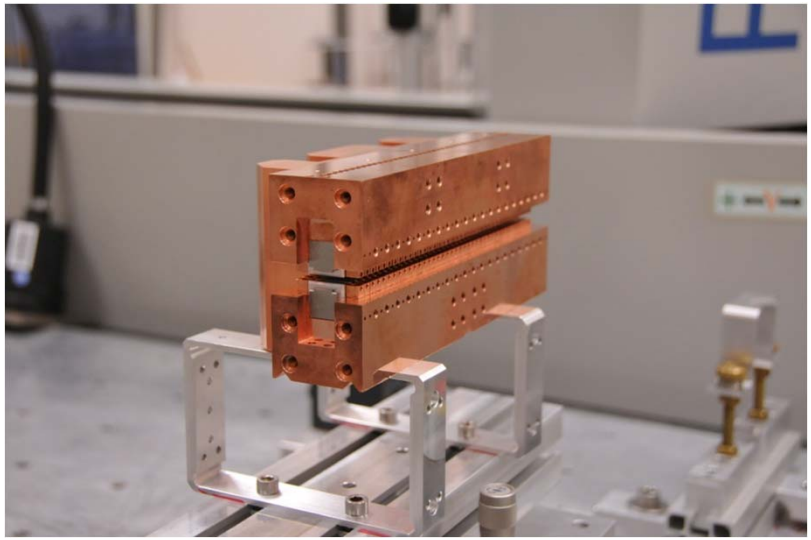

Field quality is determined
by geometric tolerances
high precision mashining required

field tuning by pole height adjustment
use of pole clamps with various heights

Cryogenics

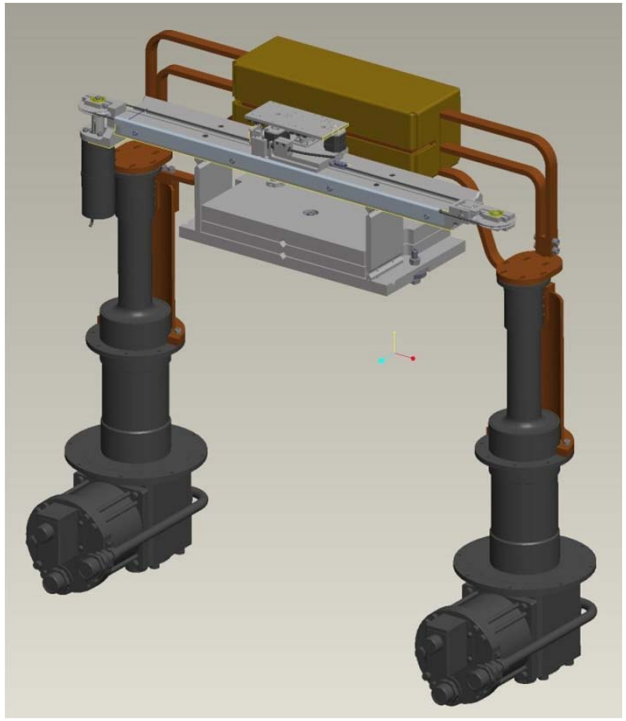

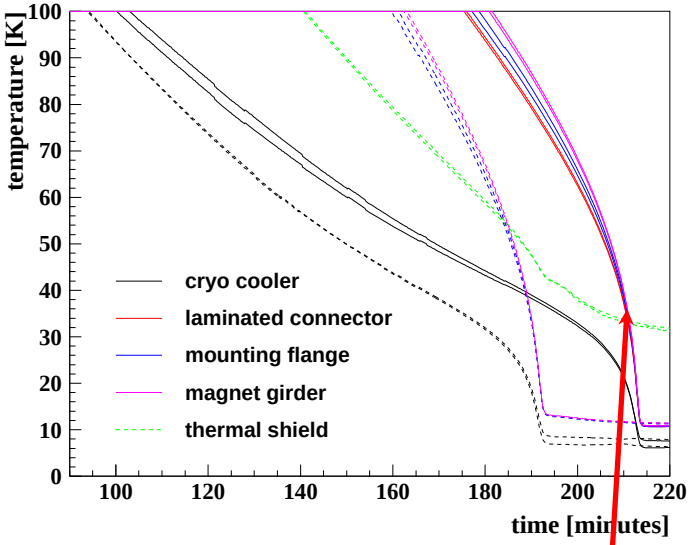

Cooling time:
3h10min without shield
2h 50min with shield
final temperature is
the same in both cases

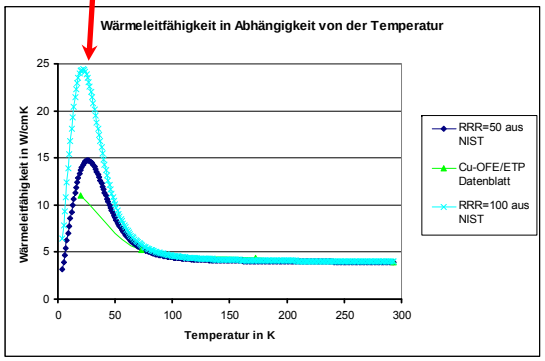

Calculated end temperature of the undulator: 17K
Measured end temperature of undulator: 11K

Reason for discrepancy is a pessimistic assumption for the Cu heat conductivity

J. Bahrdt et al., SRI 2009, AIP Conf. proc. 1234, p499-502

Radiation Hardness and Temperature

Mechanism of reversible demagnetization:

- Local heating (at grain boundaries) above critical temperature
- Demagnetzation of single domain and subsequent flip of the whole grain (nucleation type magnets)

Cryogenic devices enhance allowed heat deposition below critical T the stability increases at lower temperatures but:

- the heat capacity decreases at low tempertatures
- high coercivity alone does not help

$$C_p(T) \sim \left(\frac{T}{T_D}\right)^3 \int_0^{\frac{\theta_D}{T}} \frac{x^4 e^x}{(e^x - 1)^2} dx$$

h $\theta_D \approx 400.$

H. Fujii et al., J. of Magnetism and Magn. Materials 70 (1987) 331-333

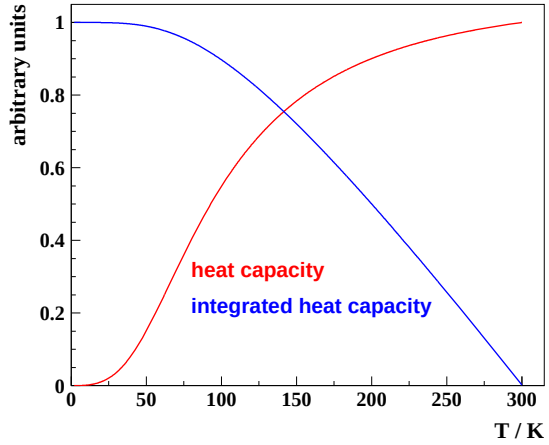

Pushing the Parameters with Shaped Poles

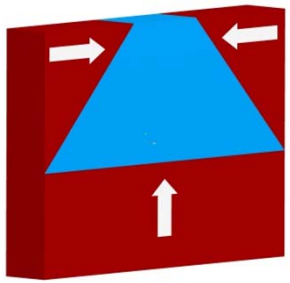

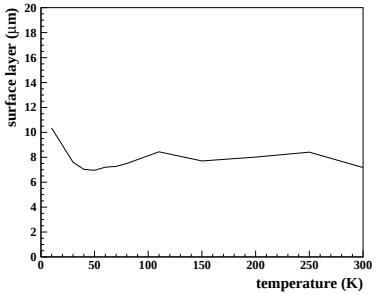

surface layer thickness: 8.5 ± 1.5µm
Slightly more than grain size

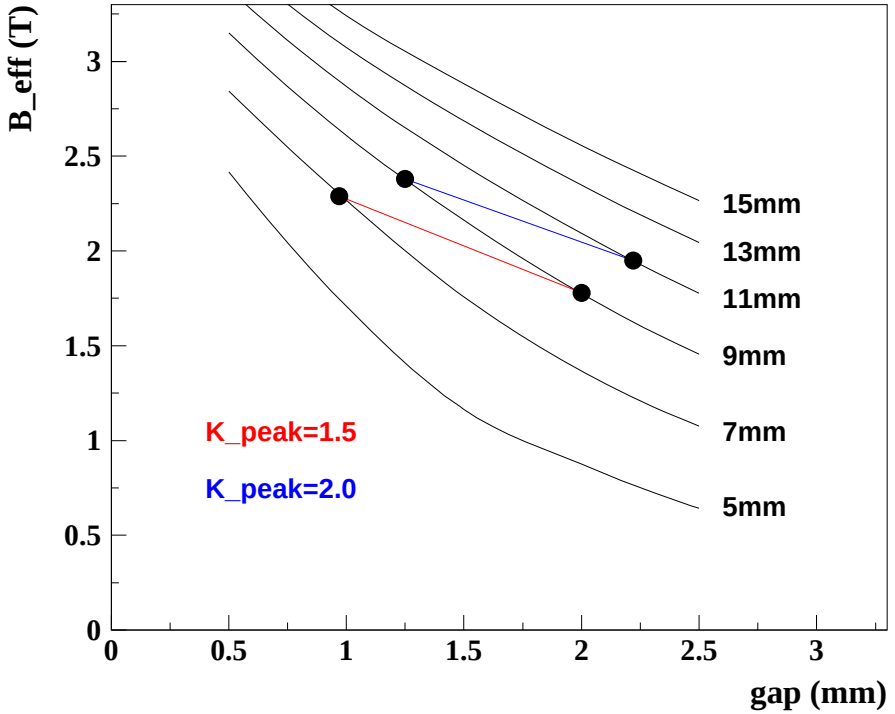

Simulations:

- minimum dead layer (9µm)
- TiN coating (3-4µm)
- tight shape tolerances (<10µm)
- small air gaps (10-20µm)

	1st prototype	*2nd prototype*
Poles	straight	transverse wedged
Period	9mm	9mm
Gap	2.5mm	1.5mm
Beff	1.15 T	1.45T @ 2.5mm 2.15T @ 1.5mm

Pole Hybrids

Substitution of part of CoFe poles with Dy or Ho

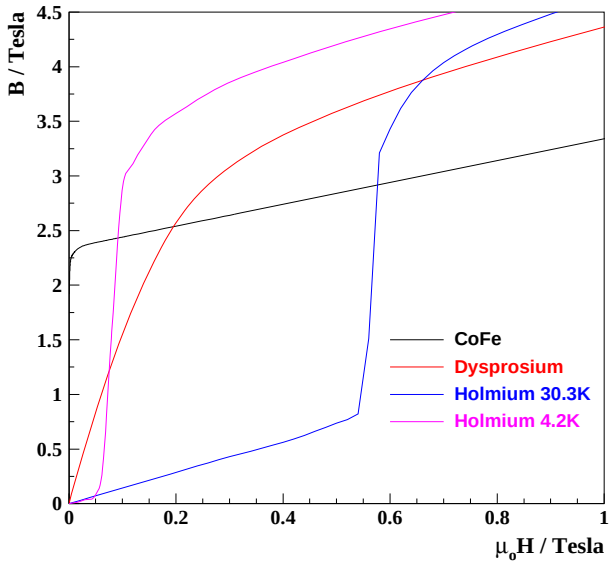

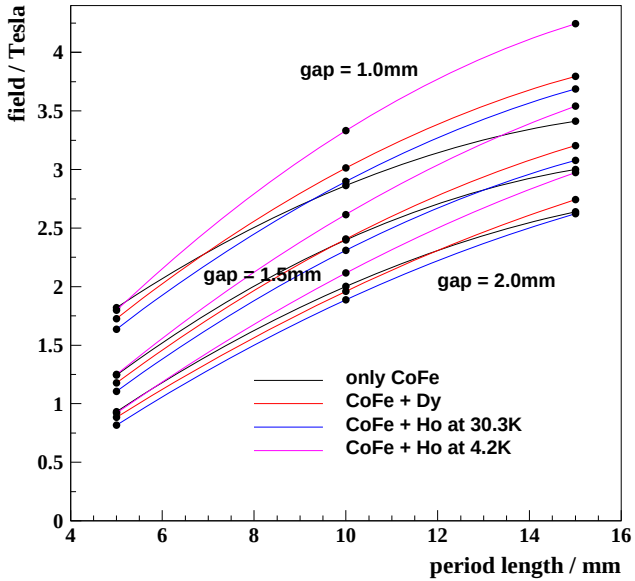

HTSC coils around pole pieces

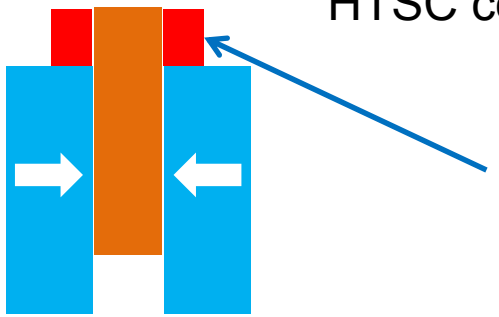

Coil support:
impregnation with resin epoxy
enhanced stability
further R & D necessary

T. Tanaka et al., New Journal of Physics, 8 (2006) 287

Pulsed Wire Systems

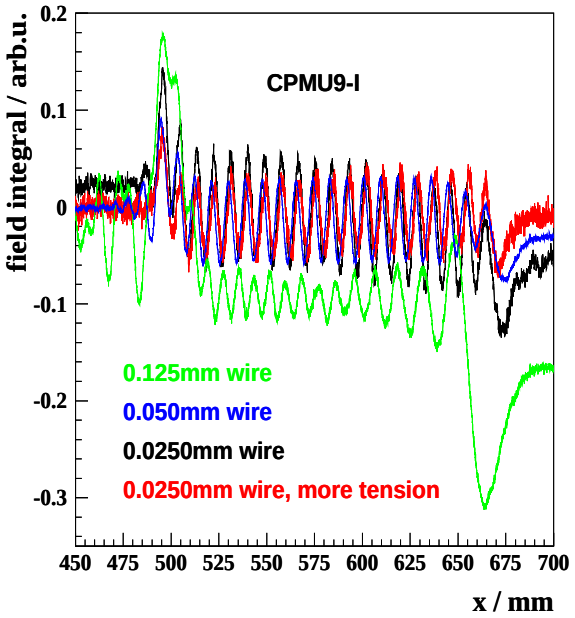

before correction

after correction

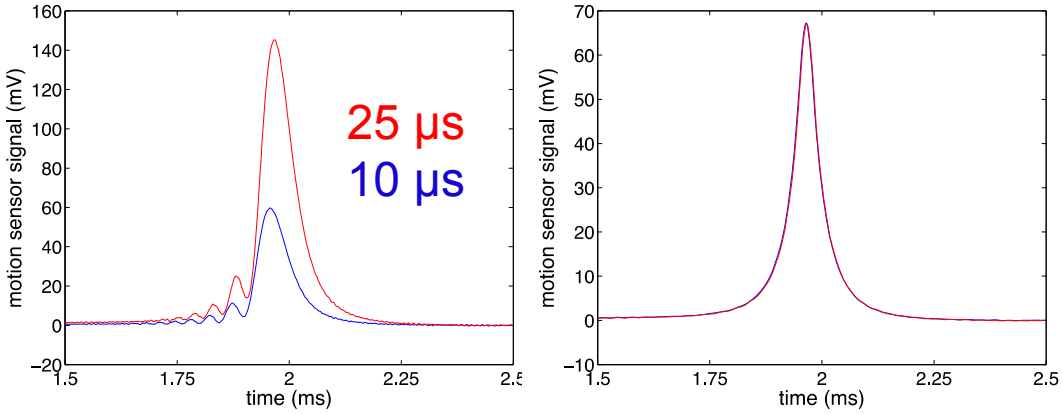

Courtesy of D. Arbelaez, LBNL

$$\rho A \frac{\partial^2 y}{\partial t^2} - T \frac{\partial^2 y}{\partial z^2} + EC \frac{\partial^4 y}{\partial z^4} = B_x I$$

$$C = \frac{\pi d^4}{64}$$

Free space propagation: $c = c_0 \sqrt{1 + \frac{EC}{T} k^2}$

$$y = e^{ik(z-ct)}$$

with $c_0 = \sqrt{\frac{T}{\rho A}}$

Numerical solution of inhomogenious time dependent differential equation

In-vacuum Hall probe Bench

HZB Helmholtz Zentrum Berlin

In-Vacumm Hall probe bench for local measurements

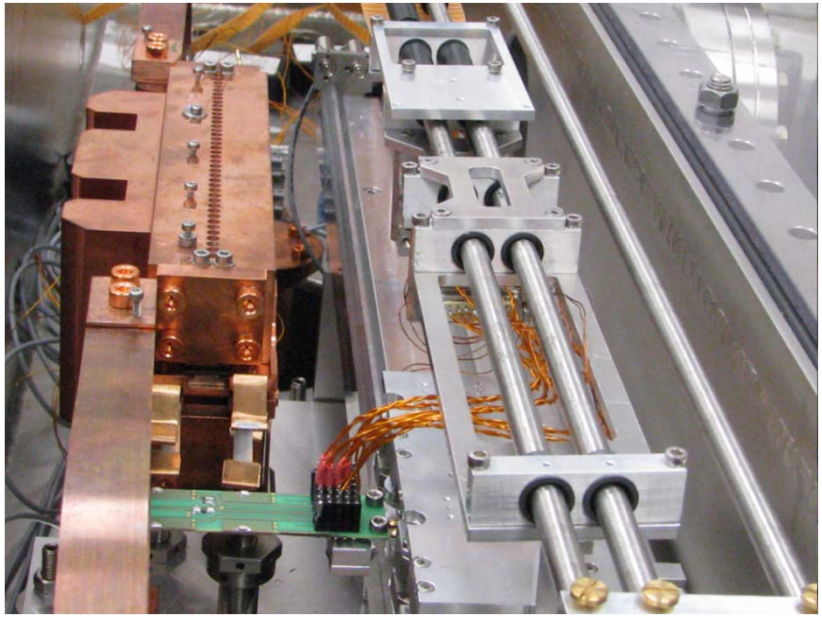

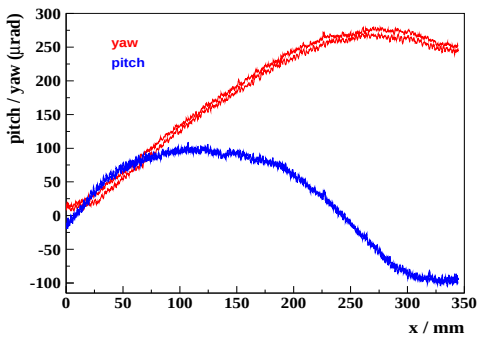

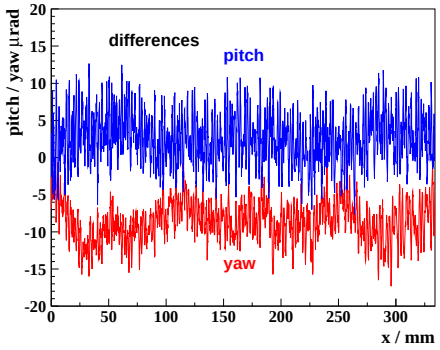

Reproducibility of sledge

Field data of 9mm prototype

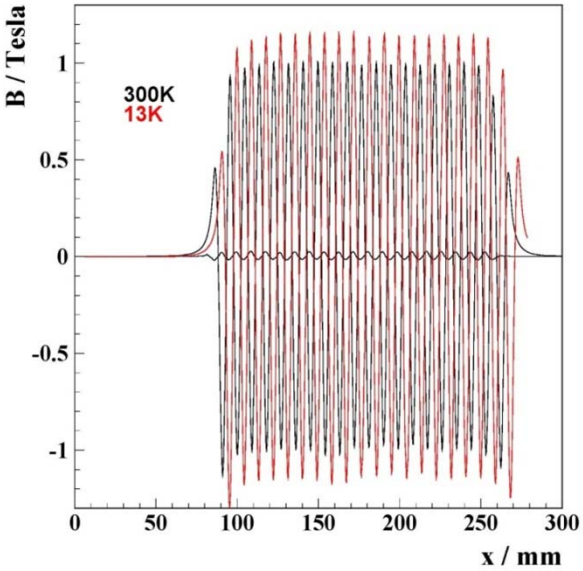

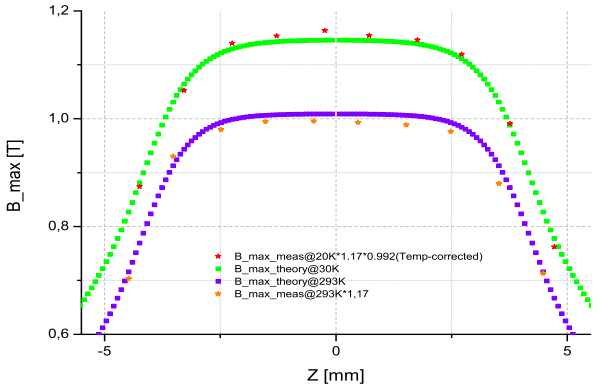

Comparison of simulation and measurement

Differences Between Room Temeprature and 15K

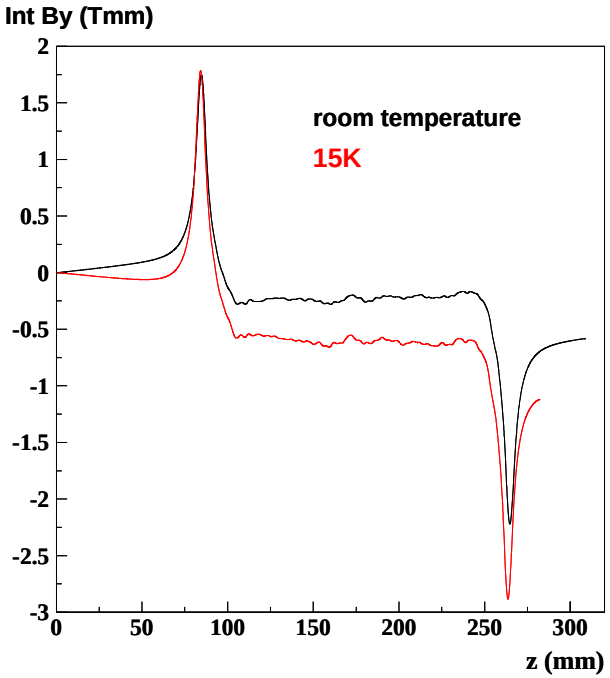

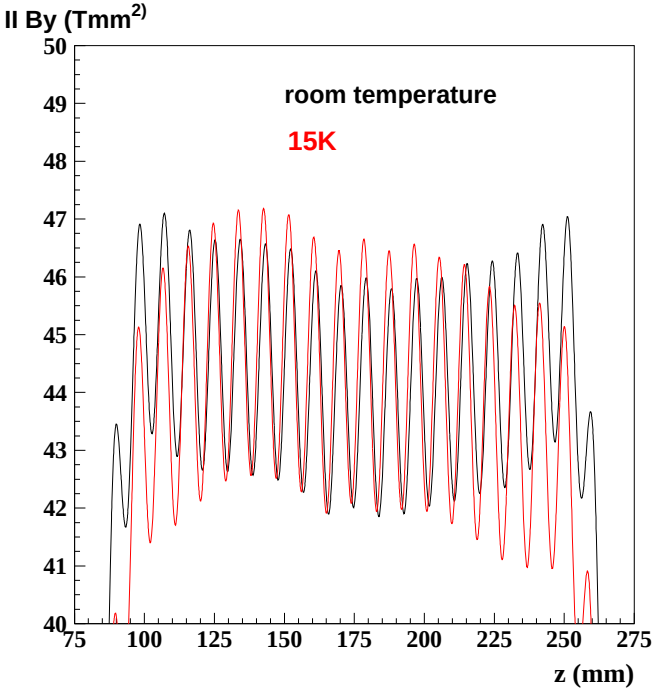

Field integral (filtered) jumps by 0.4Tmm due to temperature dependent partial saturation of endpoles

2nd field integral considerable deviations observed only at the ends

Precise analysis requires HP-calibration (T-dependent)
- HP-temperature at 15K: room temperature -15K

Conclusion

Higher fields possible with

- Cryogenic temperatures
- New materials, PrFeB, GBD
- Ambitious magnet designs, narrow good field region

Magnetic quality assurence with improved systems

- pulsed wire, correcting for dispersion
- In-vacuum Hall probe bench

Mechanic challenges

- Tighter fabrication tolerances
- Advanced gap measurement systems
- Careful cryogenic design